International Conference on Mathematics, Computational Methods & Reactor Physics (M&C 2009)
Saratoga Springs, New York, May 3-7, 2009, on CD-ROM, American Nuclear Society, LaGrange Park, IL (2009)

ORDER-OF-CONVERGENCE STUDY OF A CONDENSED-HISTORY ALGORITHM IMPLEMENTATION

Rodney L. Keith and Ronald P. Kensek
Sandia National Laboratories
P.O. Box 5800, MS 1179
Albuquerque, NM 87185
rlkeith@sandia.gov; rpkense@sandia.gov

ABSTRACT

An order-of-convergence (with respect to a path-length parameter) verification study is undertaken for an implementation of the condensed-history algorithm in a Monte Carlo electron transport code. "Condensed-history" refers to simulating the cumulative effects of the electron without modeling each individual collision. A 1992 paper by Larsen derived the expected order of convergence for a few mathematical models of this type of algorithm. We examine the order of convergence of a condensed-history algorithm based on that used in the Integrated TIGER Series (as applied to electron albedo problems) in the presence of Monte Carlo uncertainty.

Key Words: Condensed history, electron transport, order of convergence

1. INTRODUCTION

Order-of-convergence studies have become a discriminating tool for code verification for finite-element programs. In this work, we perform an order-of-convergence study on a Monte Carlo algorithm, in particular a condensed-history model of electron transport. “Condensed history” [1] refers to simulating the cumulative effects of an electron over a path-length (s) without modeling each individual collision. Larsen [2] derived orders of convergence for a few different types of condensed-history algorithms using an operator-split procedure.

This work is part of the verification activities for the Integrated TIGER Series (ITS 6) [3], a coupled electron-photon transport Monte Carlo code. The ITS condensed-history implementation uses the simplest form of electron transport (hinge at the end) [4] which, according to Larsen [2], should exhibit linear convergence with respect to path-length size.

Section 2 describes the ITS algorithm and simplifications for this study. Section 3 describes how the study was performed and what statistically valid statements can be made. We wrap up with conclusions in Section 4.

Throughout this paper, the application is the electron albedo (reflected number fraction) for a 1 MeV beam of electrons normally incident on a slab of beryllium. A sufficient number of histories were simulated so that the Monte Carlo statistical uncertainties were less than 0.5%. The slab thickness (10 cm) is much greater than the maximum electron range.

2. The ITS Condensed-History Algorithm

The main thrust of our work was to investigate the convergence properties of ITS as the pathlength ("substep size" in ITS terminology) was decreased. In fact, the unmodified ITS fails such a study as Fig. 1 indicates. The pathlength is plotted as fractions of the ITS step size, which was not altered (the default substep size for beryllium is 1/2 step).

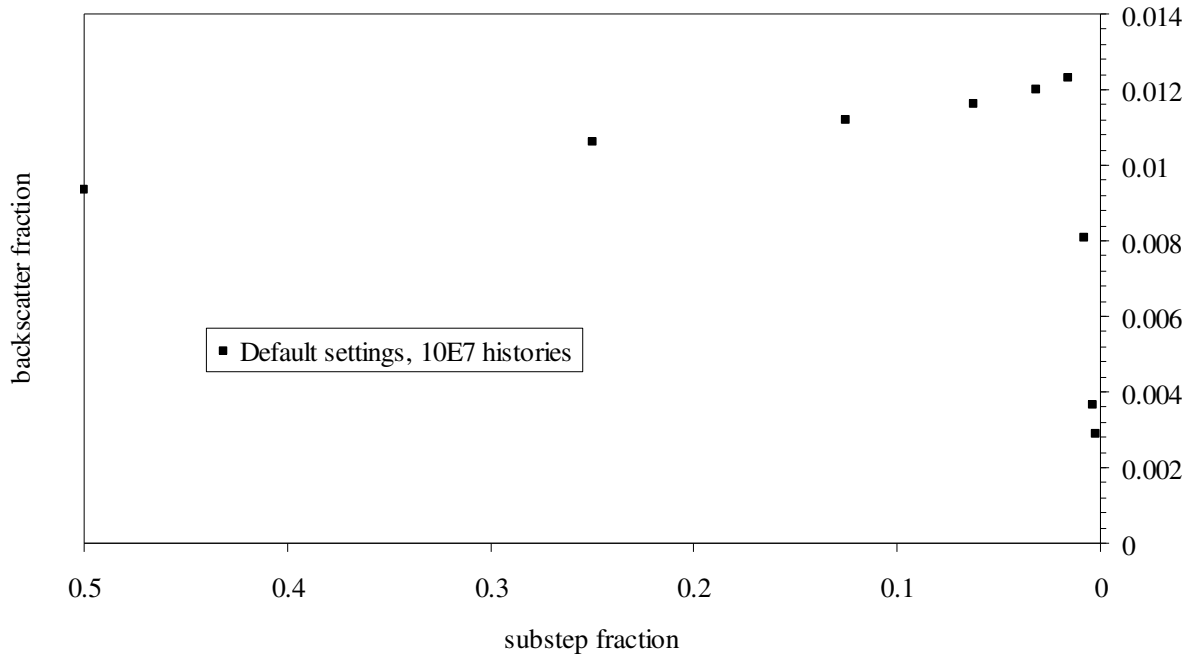

Figure 1. Backscatter results for a 1.0 MeV e^- beam on beryllium from 1/2 to 1/512 step.

To understand this failure, we review the ITS condensed-history algorithm, which makes use of the Goudsmit-Saunderson multiple-scattering distribution. This distribution has the form of a Legendre series

$$F_{GS}(\theta,s) = \sum_{l=0}^{\infty} (l+1/2)\, e^{-sG_l} P_l(\cos\theta) \tag{1}$$

where s is the pathlength, P_l are the Legendre polynomials, and the transport moments G_l are defined as

$$G_l = 2\pi N \int_{-1}^{+1} \frac{d\sigma}{d\Omega} \left[1 - P_l(\cos\theta)\right] d(\cos\theta) \tag{2}$$

The single-scattering cross section is represented by $d\sigma/d\Omega$ and N is the number of atoms per unit volume.

The computer algorithm for Eq. (1) sums to a finite number of terms l_{MAX} (treating the last term as the probability of no-scattering) and currently uses recursion relations (based on the functional form used for the single-scattering cross section) in Eq. (2) that are known to be unstable [5]. Error is controlled with an historic prescription [5] which limits the number of terms and may switch to backward recursion. However, this prescription was likely never meant to be used in a substep study.

In order to understand the failure in Fig. 1, eventually improve the code, and demonstrate linear convergence, a number of modifications were made to the ITS cross-section generating program XGEN:

- Increase l_{MAX} (the number of terms in the series). We monitored for artifacts due to instabilities by examining the transport moments (Eq. (2)) and the coefficients of Eq. (1). We also used forward recursion relations throughout, in part for simplicity but also to aid in seeing the influence of the instabilities. The instability can in principle disappear by switching to numerical integration since the recursion relations for the Legendre polynomials are known to be stable. While we have demonstrated this with various numerical quadrature routines, the run-time cost was prohibitive for a general solution.

- Increase the histogram resolution of the stored multiple-scattering distribution. As the pathlength decreases in size, the distribution becomes much more forward peaked, so additional angular bins were added between zero and three degrees.

- Use screened-Mott cross sections only. This was solely for simplification.

- Energy loss along the pathlength is treated separately (the present ITS algorithm averages the energy dependence of the transport moments over the substep), again in part for simplicity and to align with Larsen's models.

We extended the number of terms from l_{MAX} = 240 to 2290. Clear evidence of divergent behavior in our model is demonstrated in Fig. 2. At low energy, the transport moments first flatten out as expected (coefficient of unscattered) before the curve suddenly takes off (the moments actually change sign). The instability having a sudden, rather than gradual, impact was not anticipated.

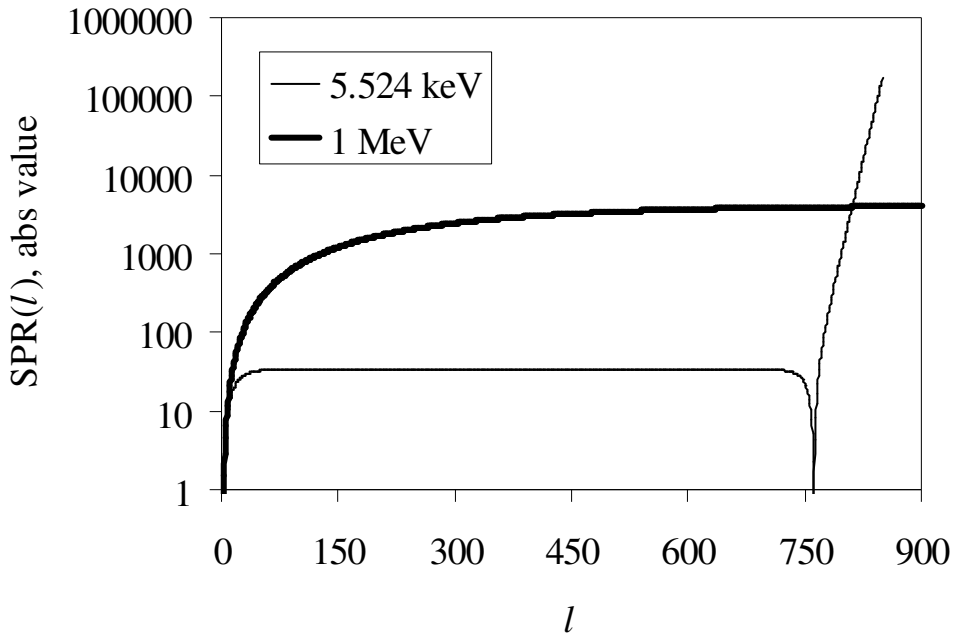

Figure 2. Divergent behavior of transport moments (G_l) at low energy (SPR = $G_l \cdot e^-$ range) for beryllium.

The need for increasing the number of terms for small substep sizes can be seen in Fig. 3, where we have plotted the angular distribution from Eq. (1) for the substep size fraction 1/512. In fact, what is plotted is $2\pi F_{GS} \sin(\theta)$ from Eq. (1) for three values of l_{MAX} : 240 (traditionally, the largest used in ITS), 1200 and 2290. The polynomial representation with 240 terms has significant portions which are negative. This both distorts the shape and makes it problematic to interpret this as a probability distribution function. If one looks closely, small high-frequency oscillations in the $l_{MAX} = 1200$ curve can be seen, though such variations may be of no consequence.

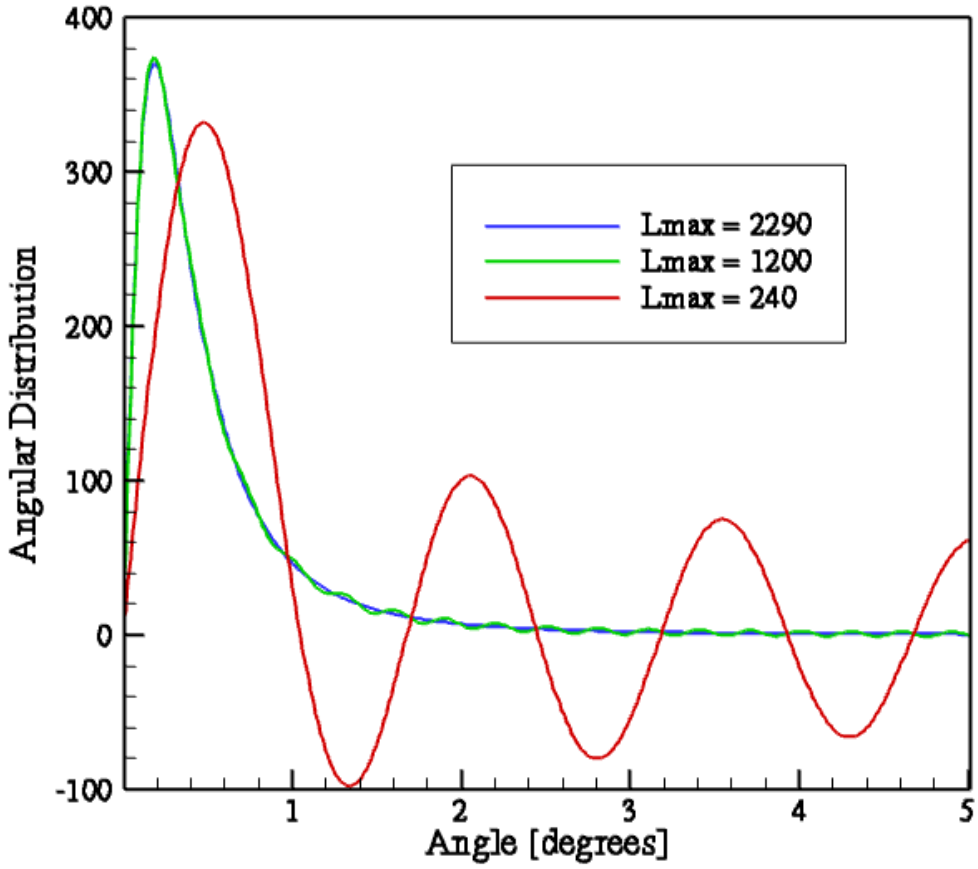

Figure 3. Legendre-polynomial representations from Eq. (1) with substep fraction 1/512, terminating the series at various numbers of terms.

Martin Berger discussed [6] and implemented [7] a scheme to separate out the uncollided and first-collided probabilities to accelerate convergence with small substeps. This is shown in Fig. 4 where the polynomial representations need far fewer terms for convergence. Already at 240 terms, the shape is much better represented. At 500 terms the small oscillations may be of little consequence. This suggests the possibility of a convergence criterion while keeping the number of terms small – in particular away from the onset of the instabilities.

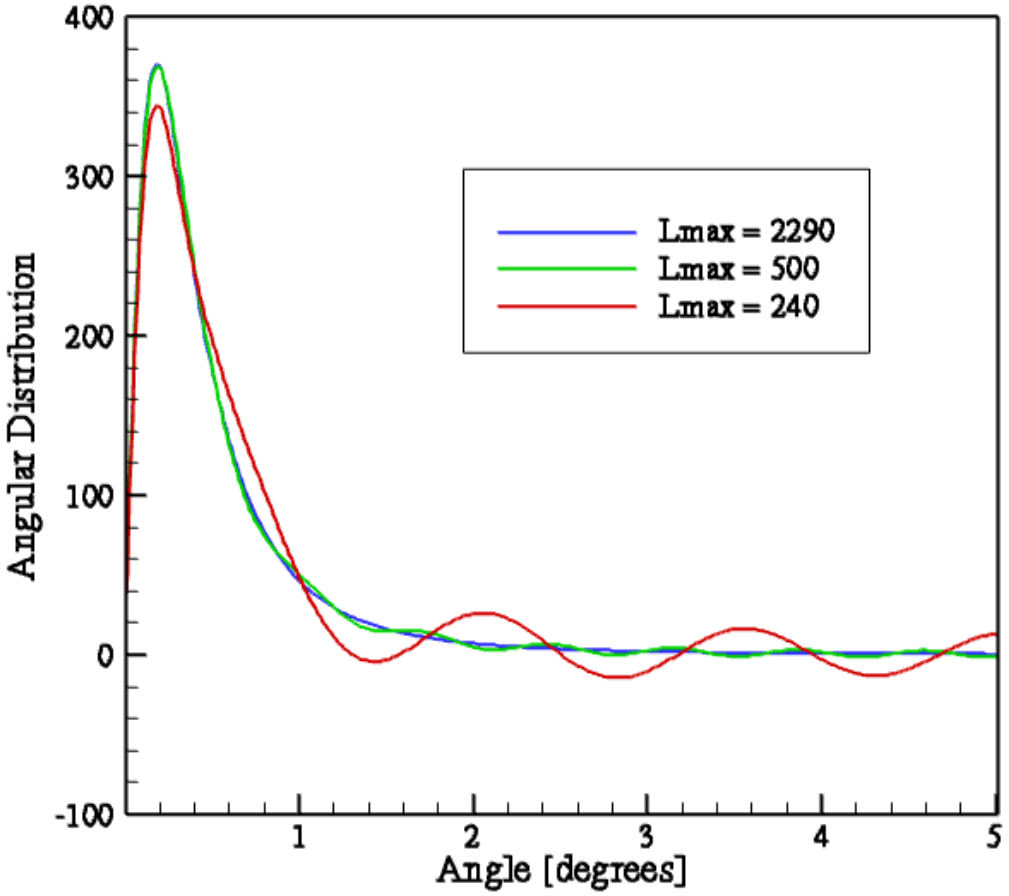

Figure 4. Representations of the multiple-scattering distribution with the uncollided and first-collided distributions calculated separately, terminating the series at various numbers of terms, for substep fraction 1/512.

3. RESULTS

The calculations were repeated with the same substep fractions, plus one additional at 1/1024, using the modifications done to XGEN and l_{MAX} = 1600 terms. The resulting plot is shown in Fig. 5. To examine how well these calculations follow the predicted linear convergence, we followed the procedure described in *Numerical Recipes* [8] for fitting a straight line to data. Linear regression was performed taking into account the Monte Carlo statistics for each calculation, all less than 0.4%. The results are shown in Table I.

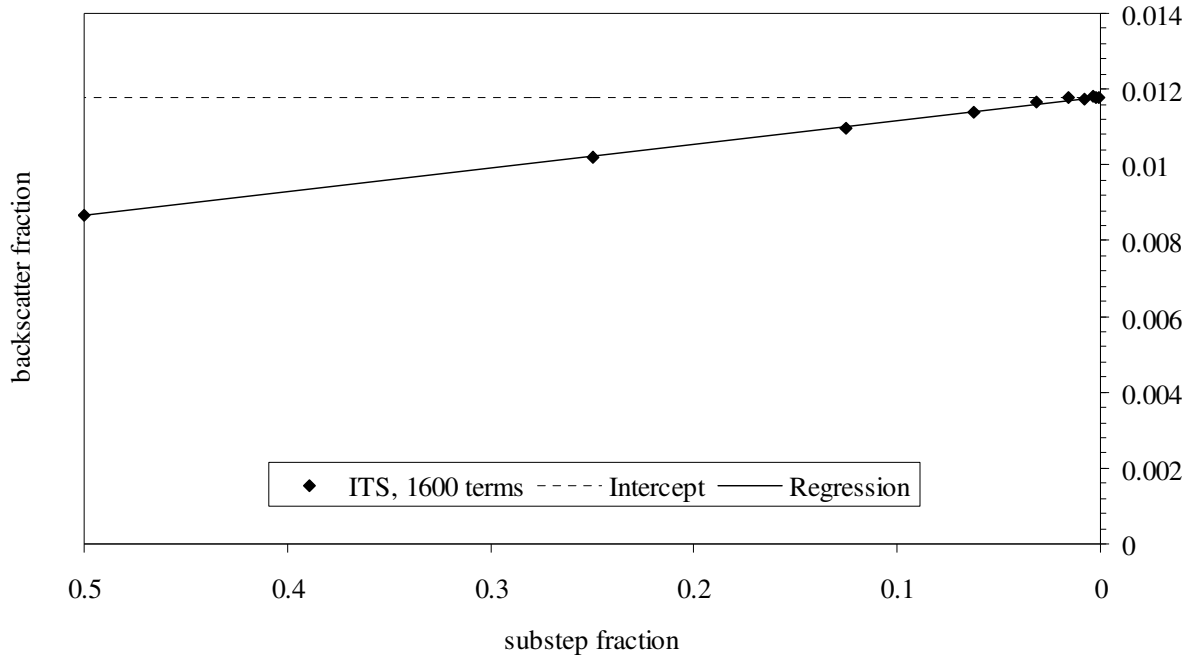

Figure 5. Backscatter results for a 1.0 MeV e^- beam on beryllium from 1/2 to 1/1024 step using all modifications. Least-squares intercept of 0.0179 included.

Table I. Least-Squares Fit Including Monte Carlo Uncertainty

	Results	**Uncertainty**
Intercept	$1.179\ 10^{-2}$	$1.216\ 10^{-5}$
Slope	$-6.274\ 10^{-3}$	$6.442\ 10^{-5}$

The regression line is also plotted in Fig. 5. A chi-square (χ^2) statistic and corresponding goodness-of-fit (Q) value were calculated. A value $\chi^2 = 8.816$ (with 8 degrees of freedom) corresponds to a Q value of 0.3580. Since $Q > 0.1$, we may claim that the calculations are statistically consistent with a linear convergence.

4. CONCLUSIONS

With a number of modifications to the cross-section generating program, we have demonstrated the order of convergence (with respect to substep size) of a condensed-history algorithm is consistent with that predicted by the theory as derived by Larsen. These modifications will be implemented in a future version of ITS, allowing more robust parameter studies on demand. Of course, in principle this can be applied to any algorithm where the order of convergence is known, such as the well-known [4] quadratic convergence of the randomly placed hinge.

The necessity of saying the results are "statistically consistent" with the known order of convergence makes this a much weaker test than that used in the finite-element (i.e. non-stochastic) analysis.

ACKNOWLEDGMENTS

Sandia is a multiprogram laboratory operated by Sandia Corporation, a Lockheed Martin Company, for the United States Department of Energy's National Nuclear Security Administration under Contract DE-AC04-94AL85000. The authors wish to acknowledge Brian C. Franke for many helpful discussions.

REFERENCES

1. M. J. Berger, "Monte Carlo Calculation of the Penetration and Diffusion of Fast Charged Particles," in *Methods of Computational Physics, Vol. 1*, Academic Press, New York, USA (1963).
2. E. W. Larsen, "A Theoretical Derivation of the Condensed History Algorithm," *Ann. Nucl. Energy*, **19**, pp. 701-714 (1992).
3. B. C. Franke, R. P. Kensek, T. W. Laub and M. J. Crawford, "ITS Version 6: The Integrated TIGER Series of Coupled Electron/Photon Monte Carlo Transport Codes," Sandia National Laboratories, Technical Report SAND2008-3331 (2008).
4. I. Kawrakow and A. F. Bielajew, "On the Condensed History Technique for Electron Transport," *Nucl. Instr. And Meth. In Phys. Res. B*, **142**, pp. 253-280 (1998).
5. S. M. Seltzer, "An Overview of ETRAN Monte Carlo Methods," in *Monte Carlo Transport of Electrons and Photons*, Plenum Press, New York, USA (1988).
6. M. J. Berger and R. Wang, "Multiple-Scattering Angular Deflections and Energy-Loss Straggling," in *Monte Carlo Transport of Electrons and Photons*, Plenum Press, New York, USA (1988).
7. M. J. Berger, "Applicability of the Condensed-Random-Walk Monte Carlo Method at Low Energies in High-Z Materials," *Radiation Physics and Chemistry*, **53**, pp. 191-203 (1998).
8. W. H. Press, B. P. Flannery, S. A. Teukolsky, and W. T. Vetterling, *Numerical Recipes: The Art of Scientific Computing (FORTRAN Version)*, Cambridge University Press, New York, USA (1989).